MODELING CASCADE PROCESSES IN TWO-DIMENSIONAL TURBULENT CONVECTION

P. G. Frik

UDC 532.517.4

The difficulty of solving equations of hydrodynamics – especially equations of thermogravitational convection – has always caused investigators to employ a two-dimensional formulation of problems whenever possible. Two-dimensional formulations have made it possible to solve many problems and have received particular impetus with the advent of numerical methods, since the examination of three-dimensional problems remains at the limit of the capabilities of modern computers even for the simplest cases. With two-dimensional formulations, numerical solutions have been obtained for nonsteady equations of natural convection in the case of Grashof numbers reaching 10^8-10^{12} [1]. This has enabled researchers to follow the evolution of the flow structure in the core and boundary layers. However, limits on the number of points and computing time have made it impossible to obtain the range of scales necessary to construct three-dimensional spectra and to examine inertial ranges. As regards turbulence, the transition to two measurements is of fundamental importance because it conserves entropy and thus retains the special properties of turbulent flows. A large number of studies have been devoted to uniform isothermal two-dimensional turbulence (see [2, 3], for example). When slight thermal irregularities not significantly affecting the fluid flow are introduced into the flow, the temperature can be regarded as a passive impurity. The spectra of this impurity for two-dimensional turbulence were studied in [4-6]. However, there has still been no study of the spectral laws in the case when the temperature from the passive impurity becomes the main source of turbulent motion. The goal of the present work is to investigate spectral processes in developed two-dimensional turbulent convection. The study is conducted on the basis of a hierarchical model of turbulence proposed in [7] and developed for the case of two-dimensional isothermal turbulence in [8]. Two-dimensional turbulence is a hypothetical phenomenon to a significant extent. Actual flows exhibiting the properties of two-dimensional turbulence are generally quasi-two-dimensional, which has an effect on their behavior. This includes flows in both the atmosphere and ocean [9] and flows of liquid metals in a magnetic field [10, 11]. The turbulence closest to being two-dimensional is probably that observed in soap films [12] and excited by the motion of a grid. In regard to examination of two-dimensional turbulent convection, it is necessary to indicate the situation in which the spectral laws being discussed might be observed. The model of developed convection in a two-dimensional formulation is familiar and convenient for experiments and theoretical studies. Convective flow in a thin vertical slit (Hele–Shaw cell) is such a model and is widely used for numerical and experimental studies of supercritical regimes of convective motion (such as in [13]). As will be shown below, the Hele–Shaw model offers one of the few possibilities of realizing developed two-dimensional turbulence containing inertial intervals under laboratory conditions.

1. Hierarchical Model of Turbulent Convection. A hierarchical model is constructed by projecting equations of hydrodynamics on a special functional basis. The model makes it possible to obtain cascade equations to describe spectral processes in a broad range of wave numbers. Construction of the model for isothermal two-dimensional turbulence was described in detail in [8]. Let us briefly discuss the principal features of the construction of a hierarchical model for turbulent convection.

We write the equations of thermal gravitational convection of a viscous incompressible fluid in dimensionless form

$$\begin{gathered}\partial \mathbf{v}/\partial t + (\mathbf{v}\nabla)\mathbf{v} = -\nabla p + \Delta \mathbf{v} + \mathrm{Gr}\xi T, \\ \partial T/\partial t + (\mathbf{v}\nabla)T = (1/\mathrm{Pr})\Delta T,\ \nabla \mathbf{v} = 0,\end{gathered} \tag{1.1}$$

where $\mathrm{Pr} = \nu/\chi$ is the Prandtl number; $\mathrm{Gr} = (g\beta/\nu^2)/\ell^3 T^*$ is the Grashof number; ξ is a unit vector directed vertically upward (along the y axis); as the units of measurement of length,

Perm. Translated from Zhurnal Prikladnoi Mekhaniki i Tekhnicheskoi Fiziki, No. 2, pp. 71-79, March-April, 1986. Original article submitted February 12, 1985.

0021-8944/86/2702-0221$12.50

TABLE 1

M									L
$N-4$	$N-3$	$N-2$	$N-1$	N	$N+1$	$N+2$	$N+3$	$N+4$	
0	0	0	0	0	0	0	0,155	0	$N+4$
0	0	0	0	0	0	0,242	0	0	$N+3$
0	0	0	0	0	0,431	0	0	0	$N+2$
−0,0088	−0,0257	−0,0796	−0,269	0	0	0	0	0	$N+1$
0	0	0	0	0	0	0	0	0	N
0,0032	0,0096	0,0269	0	0	0	0	0	0	$N-1$
0	0	0	0	0	0	0	0	0	$N-2$

time, velocity, pressure, and temperature we chose ℓ, ℓ^2/ν, ν/ℓ, $\rho\nu^2/\ell^2$, T*. The velocity and temperature are expanded in basis functions describing a set of eddies of different scales:

$$\mathbf{v}(\mathbf{r},t)=\sum_{N,n}A_{Nn}(t)\,\mathbf{v}_{Nn}(\mathbf{r}-\mathbf{r}_{Nn}),\ T(\mathbf{r},t)=\sum_{N,n}C_{Nn}(t)\,T_{Nn}(\mathbf{r}-\mathbf{r}_{Nn}), \tag{1.2}$$

where N is the number of the stage, determining the size of the eddy; the number n determines the position of the eddy in space ($\mathbf{r}_{Nn}$ is the radius vector of the center of the eddy). The eddies of the N-th stage are dispersed in space with the density $\rho_N = (3\pi/4)2^{2N}$ and in terms of size are twice as large as the eddy of the stage N + 1.

A distinctive feature of basis functions is that the Fourier transforms of functions of different stages do not overlap in the wave-number space. The functions are localized in r- and k-spaces. The explicit form of the functions is

$$\mathbf{v}_{Nn}=\frac{(\mathbf{r}-\mathbf{r}_{Nn})\times\mathbf{e}}{\sqrt{3\pi}\,|\mathbf{r}-\mathbf{r}_{Nn}|}\,\frac{(J_0(2s)-J_0(s))}{s},\qquad T_{Nn}=2^N\sqrt{\frac{\pi}{3}}\,\frac{(2J_1(2s)-J_1(s))}{s}, \tag{1.3}$$

where $s = \pi 2^N|\mathbf{r}_{Nn} - \mathbf{r}|$; **e** is a unit vector normal to the plane being examined; J_0 and J_1 are Bessel functions.

Equations (1.1) projected on basis (1.2) give us a system of equations for the coefficients A_{Nn} and C_{Nn}. To obtain a small-parameter model, it is necessary to change over to the system of equations for the mean (with respect to the stage) values of A_N and C_N ($A_N^2 = \langle A_{Nn}^2\rangle$, $C_N^2 = \langle C_{Nn}^2\rangle$

$$\frac{dA_N}{dt}=\sum_M\sum_{L>M}T_{NML}A_MA_L+K_NA_N+\mathrm{Gr}\,F_NC_N; \tag{1.4}$$

$$\frac{dC_N}{dt}=\sum_M\sum_L H_{NML}A_MC_L+\frac{K_N}{\mathrm{Pr}}C_N, \tag{1.5}$$

where $K_N = -21.4\cdot 2^{2N}$; $F_N = 3.3\cdot 2^N$.

Nonlinear terms play the main role in spectral transport, these terms being represented in the model equations by the matrices T_{NML} and H_{NML}. The procedure of obtaining these matrices is the main step in the construction of the model and was examined in detail in [8] for the matrix T. The method used to obtain the matrix H is similar. Table 1 shows the central part of the matrix T, while Table 2 shows the matrix H for N = 0. The elements of the matrix for $N \neq 0$ are determined from the relations

$$T_{NML}=2^NT_{0,M-N,L-N},\quad H_{NML}=2^NH_{0,M-N,L-N}.$$

TABLE 2

M									L
$N-4$	$N-3$	$N-2$	$N-1$	N	$N+1$	$N+2$	$N+3$	$N+4$	
0	0	0	0	0	0	0	−0,0537	−2,99	$N+4$
0	0	0	0	0	0	−0,0941	−1,49	−0,154	$N+3$
0	0	0	0	0	−0,125	−0,720	−0,153	0	$N+2$
−0,00584	−0,0145	−0,0374	−0,0996	−0,221	−0,365	−0,145	0	0	$N+1$
0	0	0	0	0	0	0	0	0	N
0,00181	0,00468	0,0125	0,0277	0,0457	0,0181	0	0	0	$N-1$
0	0	0	0,00196	0,0113	0,00239	0	0	0	$N-2$
0	0	0	0,000184	0,00291	0,000300	0	0	0	$N-3$
0	0	0	0,000013	0,000731	0,000038	0	0	0	$N-4$

One important difference in the form of the matrices is connected with the fact that the matrix T describes the spectral transport of the energy of the velocity pulsations by the velocity field itself and permits convolution relative to the diagonal M = L. Meanwhile, both the temperature field and the velocity field participate in energy transport in the case of the temperature pulsations, which makes it impossible to convolute the matrix H and leads to nontrivial diagonals M = L and M = N. Let us write Eqs. (1.4) and (1.5) in a form convenient for analysis and numerical solution:

$$\frac{dA_N}{dt} = \sum_{l=1}^{l_{\max}} (T_{N,N-l-1,N-1}A_{N-l-1}A_{N-1} + T_{N,N-l,N+1}A_{N-l}A_{N+1} + T_{N,N+l,N+l+1}A_{N+l}A_{N+l+1}) + K_N A_N + \mathrm{Gr}\, F_N C_N; \quad (1.6)$$

$$\frac{dC_N}{dt} = \sum_m \sum_{l=1}^{l_{\max}} H_{N,N-m,N-l}\left(A_{N-m}C_{N-l} - 2^{3l}A_{N+l-m}C_{N+l}\right) + \frac{K_N}{\mathrm{Pr}} C_N. \quad (1.7)$$

An increase in $\ell_{\max}$ corresponds to allowance for the interaction of increasingly distant stages. In the numerical experiments, $\ell_{\max}$ ranges from 5 to 10.

As other approaches to the study of spectral characteristics of turbulence, the hierarchical model rests on the notion of homogeneous turbulence. Thus, the question of boundary conditions is not discussed below except for the conditions on the lateral walls of the Hele-Shaw cell.

2. Passive Impurity in Two-Dimensional Turbulence. In the case of small Grashof numbers, temperature behaves as a passive impurity. This makes it possible to compare the results obtained here with well-known data on the evolution of the spectra of a passive impurity in two-dimensional turbulence.

With small Gr, the coefficients C_N do not affect the behavior of A_N, and Eq. (1.6) retains two steady-state solutions

$$A_N = A_0 2^{-N/3} \text{ and } A_N = A_0 2^{-N}, \quad (2.1)$$

corresponding to inertial intervals of transport of energy and entropy, where the energy spectrum respectively satisfies the laws [2]

$$E(k) = C\varepsilon^{2/3}k^{-5/3} \text{ and } E(k) = C_\omega \varepsilon_\omega^{2/3} k^{-3}.$$

with the constants C = 1.55 and C_ω = 1.36 [8]. Two inertial intervals can be observed in a turbulent flow supplied with energy at a certain intermediate value of the wave numbers k_0 (Fig. 1, which shows a composite graph of the spectral laws with small Gr and different Pr). The numbers next to the lines in Figs. 1-4 correspond to the powers of the wave numbers k in the spectral regions.

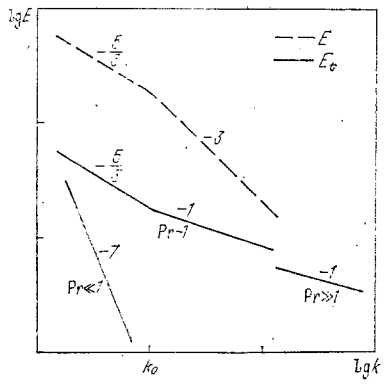

Fig. 1

In the inertial-convective range, Eq. (1.7) gives a steady-state solution $C_N = C_0 2^{-4N/3}$ in the inertial energy interval, depending on the behavior of the coefficients A_N (2.1). This solution corresponds to the spectrum of the temperature-pulsation energy

$$E_t(k) = B\varepsilon_t \varepsilon^{-1/3} k^{-5/3}, \tag{2.2}$$

while in the inertial entropy interval $C_N = C_0 2^{-N}$, which gives the following for the temperature-pulsation spectrum:

$$E_t(k) = B_\omega \varepsilon_t \varepsilon_\omega^{-1/3} k^{-1}. \tag{2.3}$$

The rate of dissipation of the temperature-pulsation energy ε_t is determined by the expression

$$\varepsilon_t = \sum_{k \geqslant N} \sum_{L<N} \sum_{M} \rho_k H_{kML} C_k A_M C_L \tag{2.4}$$

and is equal to $1.76 A_0 C_0^2$ with spectrum (2.2) and $3.1 A_0 C_0^2$ with spectrum (2.3), which corresponds to values of the constant $B = 0.5$ and $B_\omega = 0.92$. Spectrum (2.3) with the constant $B_\omega = 1.56$ was obtained in [4] in a numerical modeling of two-dimensional turbulence with a passive impurity.

The temperature cascade is preserved in the viscous-convective interval realized at large Prandtl numbers, while the corresponding velocity scales are suppressed by viscosity, and only large-scale motion is significant. Considering that only A_0 is nontrivial and that $C_N = C_0 2^{-\theta N}$, we write (1.7) in the form

$$\frac{dC_N}{dt} = A_0 C_0 2^{N(1-\theta)} \left(2^{\theta} H_{0,-N,-1} - 2^{-\theta} H_{0,-N,1}\right).$$

A steady state is possible at $H_{0,-N,-1}/H_{0,-N,1} = 2^{2\theta}$. It is evident from the matrix H (see Table 2) that the value of θ approaches $\theta = 1$ with an increase in N. This is confirmed by numerical modeling of the viscous-convective interval (Gr = 0, Pr = 1000, $\ell_{max} = 10$). Thus, the temperature-pulsation energy spectrum in the viscous-convective interval also satisfies the law

$$E_t(k) \sim k^{-1}. \tag{2.5}$$

In the inertial-diffusive interval (low Prandtl numbers), the velocity cascade is preserved, but thermal diffusion is significant. This makes the diffusion term dependent on time, a situation which in (1.7) leads to the equation

$$\sum H_{NM0} A_M C_0 + K_N C_N = 0.$$

Only the diagonal M = N = 0 is significant in the matrix, while for C_N we obtain

$$C_N = 2^{-N} C_0 A_0 H_{0,0,-N} \sim 2^{-4N},$$

which gives the spectrum

$$E_t(k) \sim k^{-7}. \tag{2.6}$$

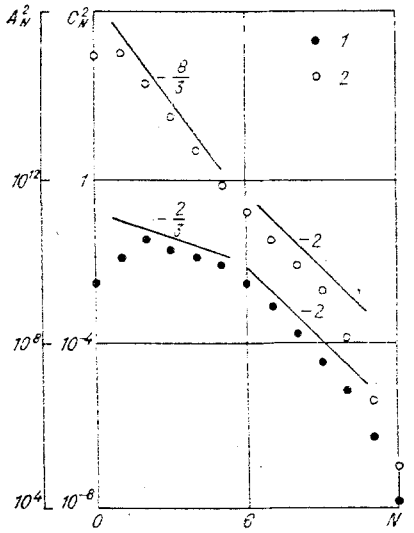

Fig. 2

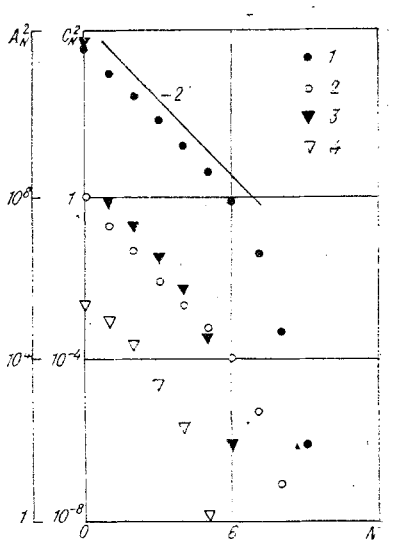

Fig. 3

Spectra (2.5) for the viscous-convective interval and (2.6) for the inertial-diffusive interval in two-dimensional turbulence were obtained from the Markov model in [5].

The behavior of a passive impurity in two-dimensional turbulence was modeled by numerically solving system (1.6)-(1.7) with Gr = 0. The number of stages ranged from 10-20 and $\ell_{max} = 10$, which corresponds to allowance for all interactions with a 1% error.

It is known from the solution of Eqs. (1.6) [8] that the steady-state solutions are unstable and that regimes (2.1) are established on the average. In obtaining the inertial energy interval characterizing the flow of energy down the spectrum, it is necessary to supply energy to a certain intermediate stage. Such a situation was modeled by solving the equations with initial conditions corresponding to concentration of the velocity and temperature pulsation energy near the fifth stage. In this case, it is possible to observe the interval $A_N^2 \sim 2^{-2N/3}$ and the corresponding value $C_N^2 \sim 2^{-8N/3}$ for $N \leq 5$. Figure 2 shows values of A_N^2 and C_N^2 averaged over time from the 1000th to the 1500th step (1, A_N^2; 2, C_N^2; Pr = 100; the time step $\tau = 10^{-8}$). An inertial entropy interval is established up the spectrum. The energy of the lower stages has increased so much by about the 5000th step that the distribution $A_N^2 \sim 2^{-2N}$, $C_N^2 \sim 2^{-2N}$ is established over the entire inviscid interval.

Figure 3 shows results of modeling of the degeneration of two-dimensional turbulence with a passive impurity. Here Pr = 1, $\tau = 10^{-8}$, and points 1 (A_N^2) and 2 (C_N^2) show mean values over time from the 1000th to the 2000th step. Energy was supplied to the bottom stage. The energy supply was cut off at the 2000th step. Points 3 and 4 give mean values of A_N^2 and C_N^2 over time from the 8000th to the 9000th step. It is evident that the energy of the lowest velocity stage even increases, while the amplitude of the remaining stages decreases by several orders of magnitude. This is the phenomenon of energy condensation in the lowest stage, which is well known for two-dimensional turbulence and in [14] was termed the δ-asymptote of the energy spectrum of two-dimensional turbulence. The amplitude of the temperature pulsations decreases smoothly.

3. Developed Turbulent Convection. It is interesting to follow the effect of convection on the spectral energy distribution. If the exponents $\varkappa$ and θ in the laws $A_N \sim 2^{-\varkappa N}$ and $C_N \sim 2^{-\theta N}$ change in the case of large Grashof numbers, then a similarity regime will no longer be assured by balancing of the corresponding triplet of terms in Eq. (1.6). Similitude can be assured only by balancing of the nonlinear terms and the term with Gr. This is possible if TNMLAMAL ~ GrFNCN, so that

$$\mathrm{Gr} \sim A_0^2,\ 2^{N(1-2\varkappa)} = 2^{N(1-\theta)}. \tag{3.1}$$

We obtain the following second condition from Eq. (1.7)

$$2^{\theta} = 2^{3-\varkappa-\theta}. \tag{3.2}$$

Comparison of (3.1) and (3.2) shows that $\varkappa = 3/5$ and $\theta = 6/5$, while the spectra must satisfy the laws

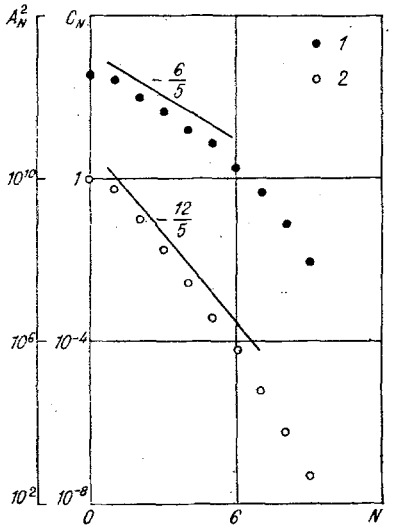

Fig. 4

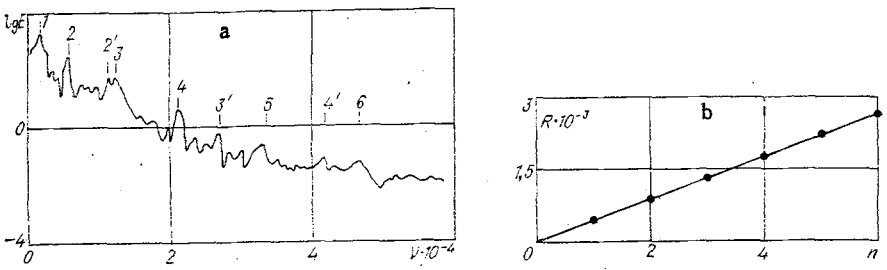

Fig. 5

$$E(k) \sim k^{-11/5}; \tag{3.3}$$

$$E_t(k) \sim k^{-7/5}. \tag{3/4}$$

Posing the question of the actual existence of two-dimensional turbulent convection containing the inertial intervals (3.3) and (3.4), let us examine quasi-two-dimensional motion in a fluid in a thin vertical plane-parallel slit with a characteristic length ℓ and distance d between the walls ($d \ll \ell$). The motion is two-dimensional ($\mathbf{v} = (v_x, v_y, 0)$), the walls are assumed to be thermally insulated, i.e., $T = \text{const}(z)$, and the velocity $\mathbf{v} = 0$ at $z = 0$ and $z = d$. Velocity is given in the form $\mathbf{v} = \mathbf{v}(x, y, t)f(z)$, while $f(z) = 6z(d - z)/d^2$. Given the above assumptions, we write the dimensionless equation for velocity, integrated over z, in the form

$$\frac{\partial \mathbf{v}}{\partial t} + \frac{6}{5}(\mathbf{v}\nabla)\mathbf{v} = -\nabla p + \Delta \mathbf{v} - D\mathbf{v} + \mathrm{Gr}\,\xi T,$$

where $D = (\ell/d)^2$.

The equation for temperature does not change with the chosen boundary conditions. The transition to the hierarchical equations causes a multiplier to appear in (1.4) in front of the matrix of nonlinear interactions. It also results in an additional term describing the friction of the fluid against the side walls. In contrast to "internal" viscosity, this friction makes an equal contribution to motion of any scale. We obtain the system

$$\frac{dA_N}{dt} = \sum \frac{6}{5} T_{NML} A_M A_L + (K_N - D) A_N + \mathrm{Gr}\, F_N C_N; \tag{3.5}$$

$$\frac{dC_N}{dt} = \sum H_{NML} A_M C_L + \frac{K_N}{\mathrm{Pr}} C_N. \tag{3.6}$$

Spectra (3.3) and (3.4) pass through Eqs. (3.5) and (3.6) just as through (1.6) and (1.7). The only question is whether or not friction against the side walls of the slit will allow turbulent flow with the spectral laws (3.3) and (3.4) to develop.

We solved system (3.5)-(3.6) with Gr = $1.5 \cdot 10^{11}$, Pr = 7, D = $5 \cdot 10^5$. There were ten stages. This corresponded to a Hele–Shaw cell with walls made of a thermally insulating material (foam plastic) with a size on the order of 1 × 1 m. The width of the slit was 5 mm. The slit was filled with water, a temperature difference on the order of 50° was imposed, and $\ell_{max} = 10$, i.e., we considered the interactions of all of the excited stages with all of the remaining stages. Energy was supplied to the zeroth stage ($C_0 = 1$).

Figure 4 shows the results of the numerical solution. Points 1 (A_N^2) and 2 (C_N^2) were averaged over the interval from the 2000th to the 5000th time step. An amplitude distribution corresponding to spectra (3.3) and (3.4) was established over the six lowest stages. In an actual flow we might expect some decrease in the energy of the higher stages due to the effect of perturbations with scales smaller than d and, moreover, having a three-dimensional structure. Nevertheless, the behavior of the low-frequency part of the spectrum in which laws (3.3) and (3.4) were obtained should not change.

As noted above, the values of A_N and C_N continuously fluctuate. This fluctuation provoked further study. To study the fluctuations of A_N and C_N, we recorded the values of these coefficients during long time intervals and subjected the results to Fourier analysis. We thereby constructed time-dependent energy spectra of pulsations of a certain scale. The spectra have a fairly complicated structure and many peaks, which is indicative of a developed stochastic regime of fluctuation.

Analysis of experimental time-spectra of the lowest spatial modes of supercritical convective flows in [15] produced a quadratic relation expressing the dependence of the frequency corresponding to the next peak on the number of the peak. It turned out that this interesting relation embraces a broad range of phenomena. The authors of [16] succeeded in observing a quadratic relation for the peaks in space–time spectra not only in supercritical fluid motions but in developed turbulent convection in closed cavities and in a Hele–Shaw MHD cell.

Analysis of the space–time spectra obtained in numerical experiments with hierarchical equations indicated their similarity to the empirical data. Figure 5a shows the time spectrum of the lowest temperature stage with the degeneration of convective motion in a Hele–Shaw cell. The numbers of the peaks are indicated on the curve. The numbers with primes pertain to multiple frequencies. Figure 5b shows the dependence of the root from the frequency $R = \sqrt{\nu_n}$, at which the peak appears on the number of the peak. The dependence confirms the quadratic nature of the relation.

It should be noted that the fluctuations of the coefficients A_N are qualitatively different in the case of isothermal turbulence. One frequency and its multiple harmonics dominate the spectrum.

We thank V. D. Zimin for his attention to the work and his useful discussions.

LITERATURE CITED

1. A. V. Buné, V. L. Gryaznov, K. G. Dubovik, and V. I. Polezhaev, "Method and program pack for numerical modeling of hydrodynamic processes on the basis of nonsteady Navier–Stokes equations," Preprint Inst. Probl. Mekh. Akad. Nauk SSSR, No. 173 (1981).
2. A. P. Mirabel' and A. S. Monin, "Two-dimensional turbulence," Usp. Mekh., 2, No. 3 (1979).
3. R. H. Kraichnan and D. Montgomery, "Two-dimensional turbulence," Rep. Prog. Phys., 43, No. 5 (1980).
4. A. P. Mirabel', "Numerical modeling of the evolution of energy spectra and the concentration field of a passive impurity in a two-dimensional turbulent flow," Izv. Akad. Nauk SSSR, Fiz. Atmos. Okeana, 10, No. 2 (1974).
5. M. Lesieur, J. Sommeria, and G. Holloway, "Zones inertielles du spectre d'un contaminant passiv en turbulence bidimensional," C. R. Acad. Sci. Paris, Ser. II, 292 (1981).
6. A. P. Mirabel' and A. S. Monin, "Statistical laws of mixing of an impurity by two-dimensional turbulence," Izv. Akad. Nauk SSSR, Fiz. Atmos. Okeana, 19, No. 9 (1983).
7. V. D. Zimin, "Hierarchical model of turbulence," Izv. Akad. Nauk SSSR, Fiz. Atmos. Okeana, 17, No. 12 (1981).
8. P. G. Frik, "Hierarchical model of two-dimensional turbulence," Magn. Gidrodin., No. 1 (1983).
9. B. A. Gavrilin, A. P. Mirabel', and A. S. Monin, "Energy spectrum of synoptic processes," Izv. Akad. Nauk SSSR, Fiz. Atmos. Okeana, 8, No. 5 (1972).

10. Yu. B. Kolesnikov and A. B. Tsinober, "Experimental study of two-dimensional turbulence behind a grid," Izv. Akad. Nauk SSSR, Mekh. Zhidk. Gaza, No. 4 (1974).
11. J. Sommeria and R. Moreau, "Why, how, and when MHD-turbulence becomes two-dimensional," J. Fluid Mech., 118 (1982).
12. Y. Couder, "Two-dimensional grid turbulence in a thin liquid film," J. Phys. (Paris) Lett., 45, No. 8 (1984).
13. D. V. Lyubimov, G. F. Putin, and V. I. Chernatynskii, "Convective motions in a Hele-Shaw cell," Dokl. Akad. Nauk SSSR, 235, No. 3 (1977).
14. A. L. Tseskis, "Two-dimensional turbulence," Zh. Eksp. Teor. Fiz., 83, No. 1 (1982).
15. G. P. Bogatyrev, V. G. Gilev, and V. D. Zimin, "Space-time spectra of stochastic oscillations in a convection cell," Pis'ma Zh. Eksp. Teor. Fiz., 32, No. 3 (1980).
16. V. A. Barannikov, G. P. Bogatyrev, V. D. Zimin, A. I. Ketov, and V. G. Shaidurov, "Laws of alternation of peaks in spectra of stochastic oscillations of hydrodynamic systems," Preprint Inst. Mekh. Sploshnykh Sred UNTs Akad. Nauk SSSR (1982).

MODELING TURBULENT TRANSFER IN A CHANNEL BY MEANS OF POINT VORTICES

P. I. Geshev and B. S. Ezdin

UDC 532.527+532.4

Much attention has recently been paid to the direct numerical modeling of turbulence. Some studies have examined three-dimensional turbulent flow in a channel at moderate Reynolds numbers Re by numerically solving the complete system of Navier–Stokes equations [1]. The main difficulty in such calculations is that motions on a scale much smaller than the distance between the nodes of the finest computing grids used in practice are important in turbulence at sufficiently large Re. Despite the increasing capacity of modern computers, the limitation on Re remains. There are other approaches to the numerical modeling of wall turbulence, such as the method of large vortices [2]. In this method, the scales of motion are divided into a calculable part (by means of "filtered" Navier–Stokes equations for large scales) and a closable, small-scale part (a one-parameter closing relation is generally used), i.e., the hypothesis of the independence of small-scale motions from large-scale motions is employed. In accordance with the principle of the similarity of turbulent flows with respect to the Reynolds number [3], the large-scale motion of a continuum away from the walls is slightly dependent on Re. Thus, it can be described by the equations of an ideal swirled fluid. In the proposed computational scheme, transverse motion is modeled by the inviscid two-dimensional motion of point vortices, while the complete Navier–Stokes equation, with a constant pressure gradient, is calculated in the mean direction of motion. Two-dimensional point vortices have been used to study mainly free flows – jets and wakes in flow about different recesses and projections. It was shown in [4] that the spectral energy flux is constant in a system of point vortices and the flow spectrum is close to a Kolmogorov spectrum. The "5/3" law follows from similarity theory in the case of isotropic turbulence. In wall turbulence, this theory leads to logarithmic velocity profiles in the region where the flow of the longitudinal component of momentum to the wall is constant [5]. Considering the successful modeling of isotropic turbulence in [4], there is hope for obtaining interesting results in wall turbulence by modeling turbulent transfer by the method of longitudinal point vortices. It was shown in the present study that such calculations give results which agree qualitatively with experimental findings; the logarithmic profiles of velocity and temperature are calculated, profiles of the Reynolds stresses and turbulent heat fluxes are obtained, and the amplitudes of fluctuating quantities are investigated. A model of turbulence based on point vortices should be considered a direct numerical model. Such an approach has an undoubted advantage, since it does not require any closing assumptions.

Novosibirsk. Translated from Zhurnal Prikladnoi Mekhaniki i Tekhnicheskoi Fiziki, No. 2, pp. 79-84, March-April, 1986. Original article submitted February 6, 1985.

0021-8944/86/2702-0228 $12.50